Application of RPMI 2650 nasal cell model to a 3D printed apparatus for the testing of drug deposition and permeation of nasal products

Elsevier Editorial System(tm) for European Journal of Pharmaceutics and Biopharmaceutics
Manuscript Draft

Manuscript Number: EJPB-D-16-00441R1

Title: Application of RPMI 2650 Nasal Cell Model to a 3D Printed Apparatus for the Testing of Drug Deposition and Permeation of Nasal Products

Article Type: Research Paper

Keywords: RPMI 2650; Transporter Expression; Nasal Permeation; Mucus; Air Liquid Interface; Primary Nasal Cells; 3D printing; Deposition; Dissolution; Permeation

Corresponding Author: Prof. Fabio Sonvico, Ph.D.

Corresponding Author's Institution: University of Parma

First Author: Michele Pozzoli

Order of Authors: Michele Pozzoli; Hui X Ong; Lucy Morgan; Maria Sukkar; Daniela Traini; Paul M Young; Fabio Sonvico

Manuscript Region of Origin: AUSTRALIA

Abstract: The aim of this study was to incorporate an optimized RPMI2650 nasal cell model into a 3D printed model of the nose to test deposition and permeation of drugs intended for use in the nose. The nasal cell model was optimized for barrier properties in terms of permeation marker and mucus production. RT-PCR was used to determine the xenobiotic transporter gene expression of RPMI 2650 cells in comparison with primary nasal cells. After 14 days in culture, the cells were shown to produce mucus, and to express trans-epithelial electrical resistance (TEER) values and sodium fluorescein permeability consistent with values reported for excised human nasal mucosa. In addition, good correlation was found between RPMI 2650 and primary nasal cells transporters expression values.
The purpose built 3D printed model of the nose takes the form of an expansion chamber with inserts for cells and an orifice for insertion of a spray drug delivery device. This model was validated against the FDA glass chamber with cascade impactors that is currently approved for studies of nasal products. No differences were found between the two apparatus.
The apparatus including the nasal cell model was used to test a commercial nasal product containing budesonide (Rhinocort, AstraZeneca, Australia). Drug deposition and transport studies on RPMI 2650 were successfully performed.
The new 3D printed apparatus that incorporate cells can be used as valid in vitro model to test nasal products in conditions that mimic the delivery from nasal devices in real life conditions.

UNIVERSITA' DEGLI STUDI DI PARMA

DIPARTIMENTO DI FARMACIA

Dear Professor Göpferich,

Please find attached a revised version of the manuscript "Application of RPMI 2650 Nasal Cell Model to a 3D Printed Apparatus for the Testing of Drug Deposition and Permeation of Nasal Products" (Ms. Ref. No EJPB-D-16-00441) taking into account all the suggestions from the reviewers.

The comments of the reviewers have been addressed and all the requested modification introduced in the revised text.

Please find here after a detailed list of the changes along with the relative comments by the two reviewers.

Kind regards,

Fabio Sonvico

UNIVERSITÀ DEGLI STUDI DI PARMA
DIPARTIMENTO DI FARMACIA
PARCO AREA DELLE SCIENZE, 27/a
43100 Parma
Tel +39-0521-905088 Fax +39-0521-905006

Answers to reviewers comments

Reviewer #1: The manuscript presented by Michele Pozzoli is very interesting, develops a novel method to determine the drug deposition, the transport studies of nasal formulations. Good correlation has been found between RPMI 2650 and primary nasal cells transporters expression values. Furthermore, the model proposed in the manuscript was validated against the FDA glass chamber with cascade impactors that is currently approved for studies of nasal products. I highly recommend the publication of this excellent work.

No modifications required.

Reviewer #4: Manuscript of Pozzoli et al. (EJPB-D-16-00441)

Pozzoli et al. developed a novel nasal model that allows assessment of deposition characteristics of nasal products as well as permeation behavior of the drugs using cultured cells. The model is very interesting; the experiments were planned and carried out carefully.

There are some points that should be addressed by the authors:

Major questions/comments:

1. Materials and methods, page 12, line 309: According to MIQE guidelines for qPCR analysis more than one housekeeping gene should be chosen. Also, it has to be verified that those genes are NOT influenced by the treatment in the chosen cells or cell line. Please comment why you did not follow this procedure and discuss this as a limitation of your study.

Ribosomal RNA, the central component of the ribosome is an abundant and one of the most conserved genes in all cells, as a consequence 18S rRNA was selected as reference gene as it is known to show less variance in expression across a wide variety of treatments when compared with other reference genes, such as ACTB and GAPDH. Recently, 18S rRNA has been indicated as the most suitable reference gene for qRT-PCR normalization of data from primary human bronchial epithelial cells infected by influenza A virus (Kuchipudi et al. Virology Journal 2012, 9:230).

In the experiments presented in this manuscript we compared gene expression for a range of human drug transporter genes between the cell line RPMI 2650 and primary nasal epithelial cells, with the aim to evidence their presence and eventual macroscopic differences.
Therefore, whilst we acknowledge that there are limitations to only using one reference gene in studies, we believe that this had no effect on the outcome or validity of the data presented in this manuscript.

A few lines justifying the choice of 18S rRNA have been added in Materials and Methods section. A statement about the limitation of this choice has been added in Results and Discussion.

2. Materials and methods, page 15, line 371 et seqq.: Did you analyze how many µg of the 96 µg spray dose were deposited on the cell inserts in the chamber? In this context please also specify what you used as the reference 100 % value to calculate percentage data in Figure 7 and Figure 8.

The amount of busesonide deposited on each cell insert was quantified as 0.79 ± 0.25 µg (mean and standard deviation of 5 replicates as suggested in comment 4). For figure 7 and 8 the 100% was calculated as the total amount of drug recovered for each well i.e. the sum of budesonide transported through, found inside and remaining on the cell layer. This has been clarified in the text at page.

3. Materials and methods, page 15, line 382 et seqq.: Please describe aspects of your analytical method in more detail. What was your lower limit of quantification? Did you use an internal or external standard? Since you mention BDP being detected at 240 nm (line 388): was that you internal standard? When was the external standard added?

The method to detect budesonide was an already validated method reported in literature; the reference was added to the bibliography (Ref 29). Linearity of the method was assessed having as lower concentration 0.1 µg/ml, i.e. the LOQ of the published method.
The reference to BDP in the text was an unintended interpolation since it was not used as internal standard in the method and was never used in the experiments presented. The text has been amended.

4. Materials and methods, page 16, line 392 et seqq.: If I see it correctly there were never more than n= 3 which representing the data population. Three replicates are alright when there is limited material. However, it is not clear why you did not perform more than three experiments, e.g. for the data represented in in Figure 7 and Figure 8, when it accounts for the major conclusions of your approach. For statistical analysis n= 3 is not really sufficient, n= 5 or 6 would be more convincing. If you only have n= 3 then you have to ensure the normal distribution of the residuals before you compare values with a statistical test. Please comment and amend.

Additional experiments of deposition/transport were performed in order to increase the number of replicates to 5 (Figure 7 and Figure 8). This changed the mean amount of busesonide deposited on each cell insert (0.79 ± 0.25 µg).

Minor questions/comments:
1. Introduction, page 3, line 81: The wording "these advantages" appears a bit odd after you discussed limitations and challenges in the preceding lines.

The text has been modified according to the suggestion.

2. Materials and methods, page 13, line 325: The printed nasal model you used is very interesting. Did you analyze the adsorption effects of budesonide to the

surface of the material? This might be a limitation of the model if strong adsorption occurs which might result in incomplete cleaning of the chamber. Please comment and discuss.

After the 3D printing process with ABS, the inner and outer surfaces of the modified chamber were treated with acetone to remove porosity, obtaining a smooth and impermeable surface. The validation process of the modified expansion chamber was aimed also to investigate the possibility of drug absorption on the plastic material. However, as showed in Table 3 no adsorption for budesonide was evidenced, as no differences in drug recovery was found between glass and plastic chamber.

3. Results and discussion, page 17, line 413 et seqq.: Please detail what you used as a qualification TEER value for your monolayers, i.e. a minimum TEER value to decide whether the monolayer was of sufficient quality for the experiments.

TEER values of 90 Ωcm^2 and above were considered good to perform experiments. This has been clarified in the text.

4. Results and discussion, page 22, line 547 et seqq.: Please detail whether budesonide has been identified as a substrate of one of the transporters that you identified.

In literature, budesonide has been shown to be substrate of P-glycoprotein (Ref 40: Inflamm Bowel Dis. 2004 Sep;10(5):578-83.). This information has been added to the text.

5. Results and discussion, page 28, line 684-686: This sentence appears to be odd with "showed" terminating the sentence.

The sentence has been modified.

Parma, 08/07/2016

Fabio Sonvico

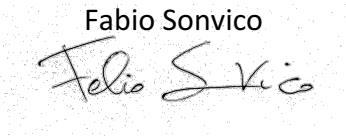

*Graphical abstract

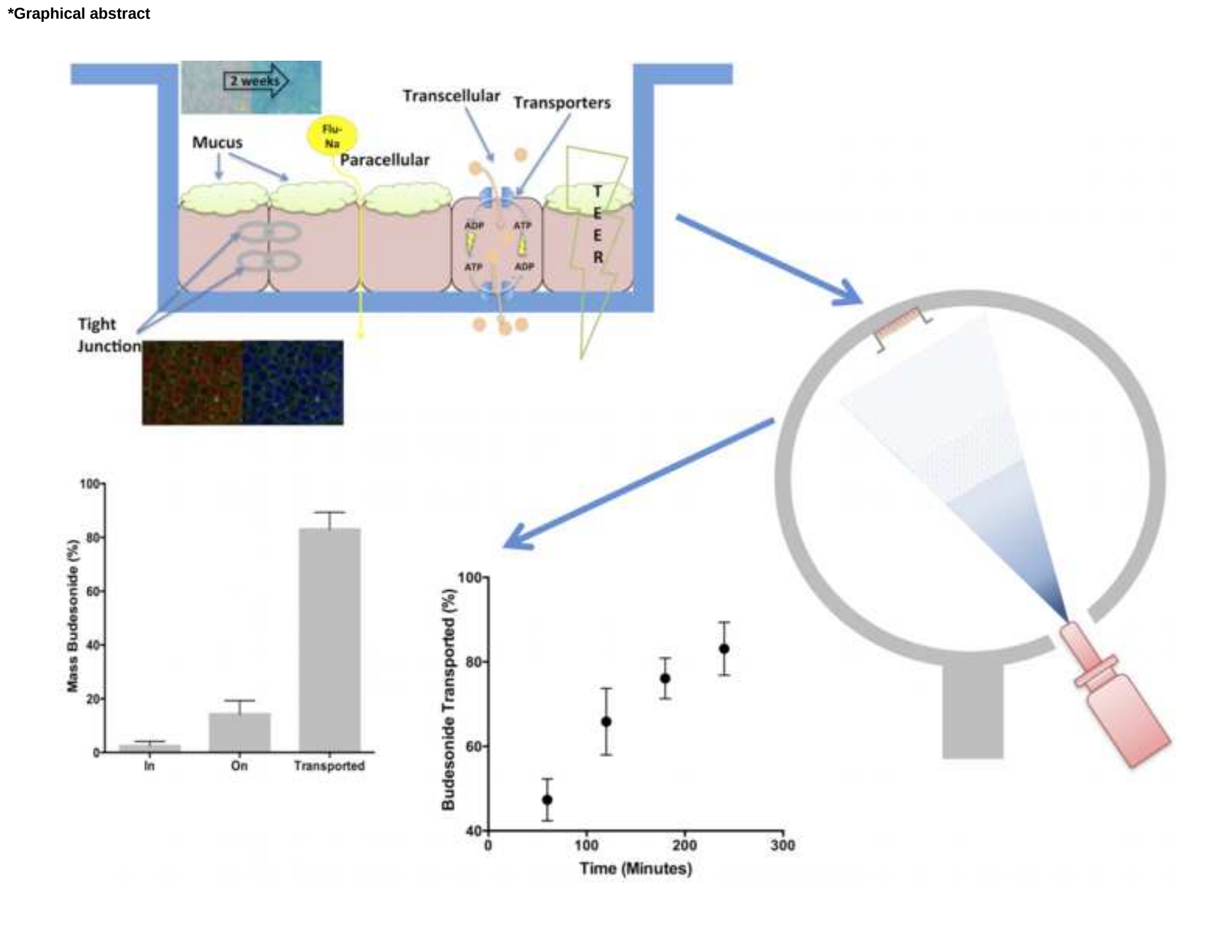

Application of RPMI 2650 Nasal Cell Model to a 3D Printed Apparatus for the Testing of Drug Deposition and Permeation of Nasal Products

Michele Pozzoli[1], Hui Xin Ong[2], Lucy Morgan[3], Maria Sukkar[1], Daniela Traini[2], Paul M Young[2], and Fabio Sonvico[1,4] *

[1] Graduate School of Health - Pharmacy
University of Technology Sydney
15 Broadway
Ultimo, NSW 2007
Australia

[2] Respiratory Technology, The Woolcock Institute of Medical Research and Discipline of Pharmacology,
Sydney Medical School, University of Sydney,
431 Glebe Point Road,
Glebe, NSW 2037
Australia

[3] Concord Repatriation General Hospital,
Sydney Medical School-Concord Clinical School,
University of Sydney,
Sydney, NSW,
Australia

[4] Department of Pharmacy
University of Parma
27A, Parco area delle Scienze
Parma, 43124
Italy
Phone: +39 0521 906282
Email: fabio.sonvico@unipr.it

*Corresponding Author

Keywords: RPMI 2650, Transporter Expression, Nasal Permeation, Mucus, Air Liquid Interface, Primary Nasal Cell, 3D printing, Deposition, Dissolution, Permeation

ABSTRACT

The aim of this study was to incorporate an optimized RPMI2650 nasal cell model into a 3D printed model of the nose to test deposition and permeation of drugs intended for use in the nose. The nasal cell model was optimized for barrier properties in terms of permeation marker and mucus production. RT-qPCR was used to determine the xenobiotic transporter gene expression of RPMI 2650 cells in comparison with primary nasal cells. After 14 days in culture, the cells were shown to produce mucus, and to express TEER (define) values and sodium fluorescein permeability consistent with values reported for excised human nasal mucosa. In addition, good correlation was found between RPMI 2650 and primary nasal cells transporters expression values.

The purpose built 3D printed model of the nose takes the form of an expansion chamber with inserts for cells and an orifice for insertion of a spray drug delivery device. This model was validated against the FDA glass chamber with cascade impactors that is currently approved for studies of nasal products. No differences were found between the two apparatus.

The apparatus including the nasal cell model was used to test a commercial nasal product containing budesonide (Rhinocort, AstraZeneca, Australia). Drug deposition and transport studies on RPMI 2650 were successfully performed.

The new 3D printed apparatus that incorporate cells can be used as valid *in vitro* model to test nasal products in conditions that mimic the delivery from nasal devices in real life conditions.

INTRODUCTION

Over recent decades, interest in the nose as an alternative site for drug administration has increased steadily [1]. The nose is attractive for drug delivery because the highly vascularised mucosa with low enzymatic activity potentiates peptide permeation and rapid, high concentration drug absorption that avoids first pass metabolism [2-6]. However, there are a number of limitations and challenges associated with nasal drug delivery. Normal mucociliary clearance would clear the nasal cavity of liquid formulations within 45 minute. The nasal cavity, even in health, is a small volume and geometrically complex space, rendered smaller by mucosal inflammation. Finally, the small volume of the cavity and the relatively low volume of fluid available for drug dissolution limits the doses that can be administered [7-10].

Together, these aspects highlight the specificity of this administration route and the need for further research into the development of new nasal formulations that are able to overcome the challenges related to efficient administration. In particular, there is an increasing need for reliable preclinical tools to screen new products and formulations intended for nasal delivery that can predict deposition and permeation through the mucosa and transport across the epithelium.

Different *in vitro* models have been proposed to investigate the deposition of nasal products. One approach is the use of transparent silicone anatomical casts such as one originated from a Japanese male cadaver Koken (Koken LM-005, Bunkyo-ku Tokyo, Japan). However, this as well as other casts,

appears to have some limitations related to the fact that the Food and Drug Administration (FDA) do not regulate the deposition experiments, each cast is not representative of the anatomical variability of different nasal cavities and its polymeric surface is far from representative of the mucosal surface present in the nose.

Another approach is to use Pharmacopoeia impactors, which have been used to predict aerodynamic particle size distributions and thus deposition profiles of aerosolized particles/droplets in the lower respiratory tract [11]. Specifically, for nasal drug delivery, the FDA guidance for industry on “Bioavailability and Bioequivalence Studies for Nasal Aerosols and Nasal Sprays for Local Action” suggests to determine particles/droplets size distribution using a cascade Impactor (CI) [12]. In particular, the guideline suggests the use of an induction port, i.e. a glass expansion chamber (EC), to be connected to a cascade impactor in order to maximise drug deposition below the top stages of the CI [11-13]. This allows a better discrimination of particles with aerodynamic diameters smaller than 10 µm that could be inhaled and therefore not suitable for the nasal deposition.

While impactors and casts are important tools to determine deposition on the different areas of the respiratory tract, they don’t offer any information related to either drug dissolution or permeation through the mucosa in the nasal cavity. Recently, various approaches that integrate lower airway epithelia cell cultures into compendia-based impactors have been proposed and used to study the deposition and permeation of particles emitted by dry powder

120 inhalers and pressurized metered dose inhalers [14-16]. To our knowledge,
121 nothing similar has been proposed for nasal products as yet.
122
123 Among the *in vitro* cell lines available commercially, RPMI 2650 is the only
124 immortalized human nasal cell line. It has been studied as a drug permeation
125 tool by different researchers [2,17-22]. Initially, it was reported that this cell
126 line was unsuitable for permeation studies because it was not able to form a
127 confluent layer in conventional culture conditions [17]. However, Bai and
128 collaborators and, two years later, Wengst and Reichel, started to further
129 investigate culture condition for this cell line and to characterize some of the
130 culture features using transepithelial electrical resistance measurements
131 (TEER), permeation of paracellular markers and tight junctions' protein
132 expression. The key findings of these studies were that the change from the
133 conventional Liquid Cover Culture (LCC) to an Air Liquid Interface cultures
134 (ALI), where the upper surface of the cells was exposed to air, was able to
135 induce cell differentiation leading to the formation of cells layers suitable for
136 permeation experiments [18,19]. A few years later, Reichel and colleagues
137 tried to optimize culturing conditions using different cell growth media and
138 different types of cell-culture insert membrane; the main studies were based
139 on TEER observation and paracellular marker permeation. A pronounced
140 dependence of TEER on medium and membrane material were observed;
141 with the best culture condition being achieved when using polyethylene
142 terephthalate (PET) 3 µm porosity Transwell™ inserts, using Minimum
143 Essential Medium (MEM) supplemented with 10% of foetal bovine serum with
144 cells cultivated using the ALI condition [21].

Based on these previous findings, the aim of the present study is to incorporate RPMI 2650 nasal cell epithelia, grown under ALI conditions into a modified expansion chamber connected to a cascade impactor. This approach, will allow the study of real nasal aerosols products, their deposition and permeation after nasal device actuation. In order to develop this new impactor/deposition apparatus, larger Snapwell™ cell culture inserts detachable from its plastic frame that can be accommodated in to the 3D apparatus without altering the aerosol performances of the impactor have been selected [14]. Firstly, the optimization of the RPMI 2650 cell line culture conditions on Snapwell inserts as nasal drug permeation model, specifically focusing on parameters that characterize the barrier properties of the model, i.e. TEER measurement, para-cellular marker permeation, tight junction localization and mucus production, were investigated. To further validate the model, a thorough analysis of the xenobiotic transporter expression in comparison with that of freshly brushed human nasal cells was carried out.

Then, RPMI 2650 grown in ALI conditions on Snapwell inserts were accommodated into a custom-built 3D printed modified expansion chamber in order to study nasal product deposition and permeation after device actuation. This new apparatus was validated against the original glass expansion chamber, recommended in the FDA guidelines, in terms of drug deposition on the CI stages and was tested in terms of drug deposition and permeation through the RPMI 2650 nasal cell model, using a commercially available budesonide nasal spray.

There is a clear need for a reliable preclinical model to test new products and formulations intended for nasal delivery that can predict drug deposition, permeation and transport across the epithelium.

MATERIALS AND METHODS

Materials

Minimum essential medium added with phenol red (MEM), non-essential amino acids solution (×100), foetal bovine serum (FBS), L-glutamine (200 mM), Hank's balanced salt solution (HBSS), TrypLE Express, bovine serum albumin (BSA) and phosphate buffered saline (PBS) were purchased from Gibco, Invitrogen (Sydney, NSW, Australia). Snapwell™ cell culture inserts (1.13 cm^2 polyester, 0.4 µm pore size) and black 96-well black plates were supplied by Corning Costar (Lowell, MA, USA). All other culture plastics were from Sarstedt (Adelaide, SA, Australia). Trypan blue solution (0.4%, w/v), paraformaldehyde and dimethyl sulfoxide (DMSO) were obtained from Sigma-Aldrich (Sydney, NSW, Australia). Fluorescein-sodium (Flu-Na) was purchased from May & Baker Ltd. (Dagenham, England). Alcian blue 1% (pH 2.5) in 3% acetic acid was purchased from Fronine laboratory (Sydney, NSW, Australia). NucleoSpin® RNA extraction kit was kindly provided by Scientifix (Cheltenham, VIC, Australia), a custom TaqMan® Array-96 well plate and all buffers where purchased by Applied Biosystem (ThermoFisher Scientific, Scoresby, VIC, Australia). Rhinocort nasal spray (AstraZeneca, North Ryde, NSW, Australia) was purchased at a local pharmacy. All chemicals and reagents were of the highest analytical grade.

194

195 **Cell Culture Nasal Cell Line**

196 The cell line RPMI 2650 (CCL-30) was purchased from the American Type
197 Cell Culture Collection (ATCC, Manassas, VA, USA). Cells between passage
198 16-30 were grown in 75 cm^2 flasks in complete Minimum Essential Medium
199 (MEM) containing 10% (v/v) foetal bovine serum, 1% (v/v) non-essential
200 amino acid solution and 2mM L-glutamine and maintained in a humidified
201 atmosphere of 95% air 5% CO_2 at 37°C. Cells were propagated and sub-
202 cultured according to ATCC protocol. The cell culture inserts were coated with
203 250µl of 1µg/ml collagen solution in PBS (rat collagen type 1 in PBS, BD
204 Biosciences, Australia) and left overnight to increase the adherence of cells to
205 the membrane [18]. In order to establish the ALI model, 200 µl of cell
206 suspension were seeded on to the collagen coated Snapwell inserts at three
207 different seeding concentrations: 1.25, 2.5, 5.0 $x10^6$ cells/ml (equivalent to
208 221, 442, 885 $x10^5$ cells/cm^2). The media on the apical compartment was
209 removed after 24 hours post-seeding. Media in the basolateral chamber was
210 replaced 3 times per week. Cell layers were allowed to grow and differentiate
211 under ALI conditions up to 21 days.

212

213 **Transepithelial electrical resistance Measurements**

214 Transepithelial electrical resistance was recorded with EVOM2® epithelial
215 voltohmmeter (World Precision Instruments, Sarasota, FL, USA) every 2-3
216 days from day one. Briefly, pre-warmed media was added to the apical
217 chamber and allowed to equilibrate for at least 30 minutes in a cell culture
218 incubator (humidified air with 5% CO_2 at 37ºC). Blank filter values were

subtracted and TEER values were calculated normalizing the resistance values with the Snapwell inserts area (1.13 cm^2).

Sodium Fluorescein Permeation Experiments

Sodium Fluorescein, a paracellular marker (Flu-Na, MW 367 Da), was used to evaluate barrier formation and tight junction functionality in the ALI culture. Three time-points were chosen to conduct the experiments (1, 2, 3 weeks) and at each time point, three Snapwell inserts were washed twice with warm HBSS before each experiment. 250 µl of 2.5 mg/ml Flu-Na solution were added to the apical chamber (donor) and 1.5 ml of pre-warmed HBSS into the basolateral chamber (acceptor). At pre-determined time points, 200 µl of solution are sampled from the acceptor chamber every 30 minutes over 4 hours and equal volume of fresh HBSS was added for replacement.

Samples were collected into a black 96-well plates and fluorescence of Flu-Na was measured with a SpectraMax M2 plate reader (Molecular Devices, Sunnyvale, CA, USA), using excitation and emission wavelengths of 485 nm and 535 nm, respectively. The calibration coefficient of determination was 0.999, with standards prepared between 1.25 and 0.0125 µg/ml.

Samples were analysed and the permeation coefficient (P_{app}) was calculated according Eq. (1):

$$P_{app} = \frac{dQ}{dt \cdot C_0 \cdot A}$$

Where dQ/dt is the flux (µg/s) of the Flu-Na across the barrier, C_0 is the initial donor concentration (µg/ml) and A is the surface area (cm^2).

242 **Evaluation of Mucus Production**

243 To assess the ability of the cell line RPMI 2650 to produce mucus when
244 cultured at the ALI configuration, Alcian Blue was used according to a
245 previously established method [23]. Mucus production of the ALI model was
246 assessed at different time points (1, 7, 14, 21 days) for three seeding
247 densities (1.25, 2.5, 5.0 $x10^6$ cells/ml), respectively. On the day of the
248 experiment, cell layers were washed twice with 300 µl of pre-warmed PBS
249 and fixed using 4% (w/v) paraformaldehyde for 20 minutes. After the fixing
250 agent was washed with PBS, the surface of the cells was stained with Alcian
251 Blue. Excess staining was washed with PBS and inserts allowed to air-dried
252 for approximately three hours. The membrane was cut from the insert and
253 mounted on to the glass slide with Entellan™ mounting medium (ProSciTech,
254 Thuringowa, QLD, Australia) and sealed. Subsequently, images were taken
255 using an Olympus BX60 (Olympus, Hamburg, Germany) microscope
256 equipped with an Olympus DP71 camera. Three images were taken per well,
257 with all conditions performed in triplicate. Images were analysed using Image
258 J software (NIH, Bethesda, MD, USA) and values of RGB (Red Green Blue)
259 were measured for each image [24]. The ratio of blue (RGBb ratio) was
260 calculated by dividing the mean RGBb by the sum of the RGB values for each
261 image (RGBr + RGBg + RGBb) [23].

262

263 **Immunocytochemistry Experiment**

264 In order to visualise the tight junction proteins on RPMI 2650 cells: ZO-1
265 (zone occluding 1) and E-cadherin immunocytochemistry was performed.
266 RPMI 2650 cells grown on Snapwell inserts for 14 days under ALI condition

were used for immunocytochemistry. The cells were washed 3 times for 30 min with PBS to decrease the amount of mucus on the cell layers and improve visualisation. Then, the cells were fixed with 4% paraformaldehyde solution for 10 min. Afterwards, the cells were incubated for 10 min in PBS containing 50 mM NH_4Cl, followed by 8 min with 0.1% (w/v) Triton X-100 in PBS for permeabilization of the cell membrane.

Cells were then incubated for 60 min with primary antibodies, i.e. 200 µL of E-cadherin (H-108) rabbit polyclonal IgG (1:100, Santa Cruz Biotechnology, Dallas, TX, USA) and ZO-1 (D7D12) rabbit monoclonal IgG (1:1000, Cell Signaling Technology, Danvers, MA, USA). Afterwards, cell monolayers were rinsed three times with PBS containing BSA 2%, before 30 minutes incubation with 200 µL of a 1:500 dilution in PBS containing 2% BSA of a goat anti-Rabbit IgG secondary antibody labelled with Alexa Fluor® 488 (LifeTechnologies, Waltham, MA, USA). 4',6-diamidino-2-phenylindole (DAPI, 1 µg/ml in PBS) was used to counterstain cell nuclei. After 30 min of incubation, the specimens were again rinsed three times with PBS containing 2% BSA and embedded in Entellan™ new mounting medium (Merk-Millipore, Darmstadt, Germany). Images were obtained using a confocal laser-scanning microscope (Nikon A1, Nikon Instruments Inc., Melville, NY, USA), using a laser at 488 nm and 60x objective.

Expression of Xenobiotic Transporters

RPMI 2650 Cell Culture and Sample Collection of Primary Nasal Cell

RPMI 2650 cells were cultured for 14 days on Snapwell porous membranes under ALI conditions at a density of 2.5 x10^6 cells/ml. To obtain primary nasal cells, bilateral nasal mucosal brushing was performed using a disposable cytology brush (Model BC-202D-2010, Olympus Australia Pty. Ltd., Notting Hill, VIC, Australia) on human subjects to collect nasal epithelium as described previously [25-28]. Samples were pooled together from eight healthy volunteers between ages 20 and 40, with two groups of four people per gender. Samples were washed and centrifuged twice with PBS solution and left in -80ºC freezer overnight prior to RNA extraction.

RNA Isolation, Target Synthesis, Microarray Data Analysis

In order to analyse the protein transporter expression in the cells samples, RNA was isolated and purified using the NucleoSpin® RNA kit (Machery-Nagel, Düren, Germany). The RNA samples were treated with RNase-free DNase sets and dissolved in RNase-free water. Concentration and purity was determined by spectrophotometry (NanoDrop 2000, ThermoFischer Scientific, Scoresby, VIC, Australia). TaqMan® Array Plates (LifeTechnologies, Sydney, NSW, Australia) was used to perform RT-qPCR assays. The array, *ad hoc* designed, enabled the assessment of 46 human drug transporter genes, including 13 ATP-binding cassette transporters, 23 solute carrier transporters, and 10 solute carrier organic anion transporters (see Table 1 for a list of all genes and proteins). Reverse transcription was carried out using a standardized internal protocol. Briefly, to 5 µl of RNA were added a mixture of general primer and deoxynucleotide (dNTP, 1:1) and 5 µl of PCR grade water; the mixture was heat at 65ºC for 5 min and quickly cooled in ice.

Subsequently, 4 µl of first strand buffer, 2 µl of 0.1 M solution of DTT (Dithiothreitol) and 1 µl of ribonuclease inhibitor were added; the solution was incubated at 37ºC for 2 minutes and 1 µl of M-MLV (Moloney Murine Leukemia Virus) reverse transcriptase was added. The mixture was incubated firstly at 25ºC for 10 minutes and then at 37ºC for 50 minutes; in order to stop the reaction the temperature was raised to 70ºC for 15 min. The cDNA for all the samples was uniformly diluted to 20 ng/µl and mixed with TaqMan® mastermix. Thermal-cycling conditions were set to manufacturer specifications, with 20 µl of mixture (sample and mastermix 1:1) were added to each well. The plates were analysed using the StepOnePlus™ Real-Time PCR System (Applied biosystem, ThermoFisher Scientific, Scoresby, VIC, Australia) for a total of 40 cycles. Data analysis was performed using the ΔCq method, where the ΔCq value is normalized to the 18S ribosomal RNA (18S rRNA) used as a reference gene. Ribosomal RNA, the central component of the ribosome is an abundant and one of the most conserved genes in all cells. Recently, 18S rRNA has been indicated as the most suitable reference gene for qRT-PCR normalization of data from primary human bronchial epithelial cells [29].

Development and Validation of Aerosol Nasal Deposition Apparatus

Development of the Modified Expansion Chamber

Rapid prototyping with 3D printing technique was used to manufacture the custom-made modified expansion chamber (MC) (Figure 1). The MC was designed to accommodate up to 3 Snapwell cell culture inserts, using CAD

341 software (Catia 3D, 3DS, Boston, MA, USA). The modified expansion
342 chamber was designed based on the 2L glass expansion chamber (EC) as
343 suggested in the FDA guidance for nasal products [12]. The MC comprises of
344 two interlocking hemispheres: the lower part presents the connection to the
345 cascade impactors (through a connection adaptor), and an inlet hole for nasal
346 devices at 30º from the axis. The upper half is designed to allow the
347 incorporation of three Snapwell cell culture inserts, located opposite to the
348 inlet hole (Figure 1).
349
350 Acrylonitrile butadiene styrene (ABS) was used as printing material using a
351 commercial 3D printer (Dimension Elite, StrataSys, Eden Praire, MN, USA), at
352 layer thickness of 178 µm. Due to the intrinsic porosity of the printed material,
353 the internal and external surfaces were chemically treated with small
354 quantities of acetone to seal internal surfaces; absence of leakage was
355 successfully tested with different mixtures of water and methanol.
356
357 (Figure 1 Here)
358
359 *Validation of the Impactor Deposition Performances: Standard vs. Modified*
360 *Expansion Chamber*
361 Rhinocort, a commercial available nasal spray for the treatment of rhinitis
362 (AstraZeneca, North Ryde, NSW, Australia), containing a suspension of
363 Budesonide (32 µg/spray) as active ingredient, was used to validate the
364 modified chamber. Aerodynamic particle size distributions were evaluated
365 using a British Pharmacopoeia Apparatus E – Next Generation Impactor

(Westech W7; Westech Scientific Instruments, Upper Stondon, UK) (Figure 2). Analyses were performed in triplicate with either the glass expansion chamber or the modified chamber fitted with Snapwell inserts. The device was primed to waste and for each analysis, three actuations were fired. Briefly, the impactor was connected to a rotary pump (Westech Scientific Instruments, Upper Stondon, UK) at a flow-rate of 15 L/min using a calibrated flow meter (Model 4040, TSI Precision Measurement Instruments, Aachen, Germany). Each impactor stage was washed with a solution 80:20 (% v/v) methanol/water and samples analysed by high performance liquid chromatography (HPLC) using a validated method [30].

(Figure 2 Here)

Validation of the Cell Layer Integrity in the Modified Chamber

RPMI 2650 were cultivated on Snapwells at the optimized seeding condition. At day 14, three cell inserts were washed with pre-warmed HBSS, and placed into the modified expansion chamber. An HBSS solution into a VP3 Aptar nasal pump (Aptar, Le Vaudreuil, France) was used as blank to simulate the deposition process into the modified chamber. After 6 actuations of the buffer blank solution, with the same deposition method previously described, the inserts were transferred into a cell culture plate. Flu-Na permeation studies were performed as mentioned above in order to confirm that the integrity of the cell layers after aerosol deposition. The P_{app} was compared with untreated control cells.

Deposition and Transport of a Commercial Budesonide Nasal Spray on Optimized RPMI 2650 cell Model using the Modified Expansion Chamber

RPMI 2650 cells were used after 14 days from seeding on Snapwells (2.5 x10^6 cells/ml). Three cell inserts were washed with pre-warmed HBSS buffer and fitted into the upper hemisphere of the modified expansion chamber. The aerosol deposition of budesonide on the cell surface from the Rhinocort device (AstraZeneca, North Ryde, NSW, Australia) was obtained according method described above, with a total dose of 96 µg of budesonide (3 sprays) was delivered into the chamber. The cell inserts were then removed from the modified chamber and transferred to a 6-well plate containing 1.5 ml of fresh pre-warmed HBBS. Samples of 200 µl were collected from the basal chamber every hour and replaced with the same volume of fresh buffer. After four hours, the apical surface of the epithelia was washed twice in order to collect any remaining drug. Subsequently, cells were scraped from the insert membrane and lysed with CelLytic™ buffer (Invitrogen, Sydney, NSW, Australia) in order to quantify the amount of budesonide inside the cells by HPLC. TEER measurements were performed prior and after the deposition in order to confirm that the integrity of the cell layer was maintained.

Analytical Quantification of Budesonide

The amount of budesonide in each sample was determined using an HPLC system equipped with a SPD-20A UV-Vis detector (Shimadzu, Tokyo, Japan) according to a validated method reported in literature [30]. Briefly, a Luna C18 column (150 X 4.6 mm, 3 µm, Phenomenex, Lane Cove, NSW, Australia) was used with a mobile phase methanol/water 80:20 % v/v. The flow rate was set

at 1 ml/min and budesonide was detected at λ=240 nm. The retention time of budesonide was around 5 minutes. Standards were prepared in the mobile phase, and 100 µl injections were used. Linearity was confirmed between 0.1 µg/ml and 50 µg/ml [30].

Statistics

Unless differently stated, data represent the mean ± standard deviation of at least three independent experiments. t-Test was used to compare data, with differences considered significant for $p < 0.05$.

RESULT AND DISCUSSION

Transepithelial Electrical Resistance (TEER) Measurements

Transepithelial electrical resistance can be used as an indicator of the development and integrity of the epithelial barrier. Various studies have tried to optimize and standardize the culture conditions of RPMI 2650 [21, 22]. However, the effects of seeding density on RPMI 2650 cultured in the ALI conditions on this Snapwell insert with a larger surface area has not been previously evaluated. The Snapwell inserts offers a more flexible membrane compared to the more common 0.33 cm^2 Transwell inserts due to their larger surface area and different support structure.

(Figure 3 Here)

The progressive formation of the tight junction barrier by cultured RPMI 2650 cells seeded onto Snapwell inserts with respect to time is shown in Figure 3. The TEER for the three different seeding densities steadily increases with time until day 14, starting from values around 20 $\Omega \cdot cm^2$ and reaching a plateau between 115 $\Omega \cdot cm^2$ ($5x10^6$ cells/ml seeding) and 150 ($1.25x10^6$ cell/ml seeding) up to day 17 when the TEER starts to decrease. Data indicate that at least 14 days are required for the cell to reach a tight confluent layer with the highest TEER barrier when cultured in the ALI conditions. After 17 days, a decrease of the TEER values is observed, suggesting that the cells either start to die or lose their tight junction integrity a few days after full maturation. This trend is similar to previously published data [21]. Regarding the three different seeding levels, no statistical differences were found at

days 14 and 17, reaching values around 90-150 Ω•cm^2. Therefore, values above 90 Ω•cm^2 were considered sufficient to perform experiments.

We report a clear correlation with the range of TEER values reported for human nasal mucosa. our results are very similar to those reported previously [18,21,31]. In particular, TEER values from excised human mucosa obtained from turbinectomy surgeries and used within an hour from the extraction, showed TEER values around 90-180 Ω•cm^2. Therefore, this data support the use of ALI cultured RMPI 2650 as a representative model of the nasal mucosa.

Sodium Fluorescein Permeation Experiments

The relatively high variability in TEER values reported in literature for RPMI 2650 cells suggests that this measurement is affected by many factors related to the technique (inter/intra laboratory), therefore other parameters have to be considered when trying to establish a model for drug deposition and transport. Thus, permeation studies of Flu-Na were performed in order to confirm and support the TEER measurements. Sodium fluorescein, due to its hydrophilic characteristic, is used as a paracellular permeation marker. The transport of Flu-Na across RPMI 2650 cell layer was evaluated over a period of 4 hours (Table 2). In order to confirm that, the Snapwell insert membrane were not the rate-limiting step of the permeation process, permeability of Flu-Na through the Snapwells membrane alone was also tested and showed a significantly higher value (1.38 x10^{-5} cm/s).

(Table 2 Here)

As shown in Table 2, no statistical difference was observed between the P_{app} values of the three different seeding densities after a week of culture, suggesting that seven days in ALI conditions are not sufficient to have a tight confluent cell layer. After 14 day of culture, the P_{app} values significantly decreased, when compared to the values of week 1, supporting the findings of the TEER experiments. It was also found that the intermediate seeding density reaches the lowest value of 2.68 ± 0.60 $x10^{-6}$ cm/s after two weeks in culture. On the other hand, the lowest seeding density (1.25 $x10^{6}$ cells/ml) shows higher permeability compared to the others two, suggesting that the amount of cell may not sufficient to guarantee enough barrier properties. No significant differences between the Papp values for the two higher seeding densities were observed. After three weeks in culture, no significant difference in the Flu-Na permeability was found for any of the seeding densities, suggesting two weeks in culture is enough to reach a mature model with confluent cells for RPMI 2650.

Different research groups have tried to characterize the paracellular permeability of RPMI 2650 grown in ALI conditions: Bai et al obtained values of $5.07x10^{-6}$ using mannitol as marker [19]; Wengst and Reichel, using Flu-Na, on cells grown on Transwell® polycarbonate membrane, presented values of $6.09x10^{-06}$ cm/s [18]; and Reichel obtained lower values of $1.91x10^{-6}$ cm/s using Thincert® inserts with polyethylene terephthalate membranes, confirming that the supporting material may affect the adhesion and the layer/barrier formation of RPMI 2650 cell line [18,21]. More recently, Kreft reported P_{app} values of $6.08x10^{-7}$ cm/s using dextran conjugated to fluorescein isothiocyanate (MW 10,000), an extremely low value that is related to the higher molecular weight of the molecule used for the investigation [20].

Evaluation of Mucus Production

Mucus plays an important role in protecting the nasal epithelium. Furthermore, this mucus is the first barrier that any drug administered into the nose has to overcome in order to be absorbed; it has a key role also in the dissolution process of drug that will allow subsequent permeation [32]. Thus, an appropriate model of the nasal epithelium requires mucus of specific depth, biochemistry and rheology. Therefore, the production of mucus in the RPMI 2650 cellular model grown in ALI condition was investigated.

Alcian Blue allows mucus detection by reaction with acidic polysaccharides (mucopolysaccharides) and sialic acid containing glycoproteins, producing a blue color. Figure 4 shows an example of the staining of the mucus layer of RPMI2650 seeded at 2.50 x10^6 cell/ml over a 3 week period.

(Figure 4 Here)

Observing the images in Figure 4 it can be seen that, after one day of culture, just few light blue spots appear, most probably due to the staining of the extracellular matrix. After one week of culture the cell layer is almost completely covered by a thin but discontinuous light blue layer, but the increased blue intensity implies that a small amount of mucus has been produced. At 14 days, the higher intensity of the colour and its uniformity suggest that the production of mucus has increased and that a mucus blanket uniformly covers the cell layer. At day 21, the mucus still cover all the area but not uniformly, dark blue areas are alternate to light ones; this could

be related to the concurrent decrease in TEER between day 14-21 suggesting cell integrity and/or death occurs.

The relative quantification of the mucus production was measured by the RGBb ratio. Figure 5 shows the mucus production in terms of RGBb ratio over three weeks. No differences in mucus production can be observed between the different seeding densities at day 1 and day 7. However, at week 2, the intermediate (2.50 $x10^6$ cell/ml) seeding shows a statistically significant increase in mucus production that was statistically higher than the other two densities. This RGBb value subsequently plateaus from day 14 to day 21. While the lowest and highest seeding densities (1.25 and 5.0 $x10^6$ cell/ml) showed no statistically differences at both day 14 and 21. These two seeding conditions showed a steady increase in the RGBb ratio value indicating a build-up in the mucus production during all the culturing time. Finally at day 21, all three seeding density managed to attain similar amount of mucus produced with no significant differences observed between them.

These results suggest that the intermediate seeding density (2.50 $x10^6$ cell/ml) is the optimum condition that allows the cells to form confluent layer with a uniform mucus blanket in 2 weeks in the Snapwell insert. This is probably due to the optimisation of the growth conditions that allow for the cells to proliferate, sufficient nutrients and space to interact and form tight junctions and produce mucus.

The plateau observed for the intermediate seeding density, can also be a result of the limitations of measurement technique leading to a saturation of the blue RGBb ratio [23]. In addition, being an *in vitro* model, one of the limitations is the static

nature of this system where the mucus cannot be cleared leading to build up in the wells with the increasing cell numbers.

Based on the above results for mucus production, TEER measurements and Flu-Na permeability, the optimal seeding density was found to be 2.50 x10^6 cell/ml for RPMI 2650 cells grown on Snapwell inserts.

(Figure 5 Here)

Immunocytochemical investigation

Tight junctions play an important role in the control of the paracellular permeation across the epithelia [33]. In order to confirm that the RPMI 2650 cells on Snapwell inserts were also able to produce tight junctions, the expression and localization of two proteins essential for the formation and maintenance of tight junction were investigated; specifically, E-cadherin and *zonula occludens* protein 1 (ZO-1) (Figure 6). Figure 6A shows the localization of E-cadherin (green) around the nucleus stained with DAPI (blue) and Figures 6B and C show in green the expression of ZO-1 and in red DAPI.

As expected, the proteins are found at the edge of the cells where they are involved in the formation of tight junction in the RPMI 2650 cells. Furthermore, the RPMI 2650 cells was found to form multilayers as seen with the overlapping nuclei in Figure 6C. This is different from what Bai et al as observed, where cells were forming a monolayer. However it is in good agreement with Kreft et al that noticed a multi-layering growth of RPMI 2650 when cultured in ALI conditions [19,20].

(Figure 6 Here)

Expression of Xenobiotic Transporters

When paracellular transport across epithelia is not involved, membrane carrier proteins can have a key role in the absorption, distribution and elimination processes of both endogenous compounds and xenobiotics [34,35]. In order to cross the epithelia a molecule needs to pass through two barriers; specifically it needs to be

taken up from apical membrane and effluxed from the basal membrane. These processes are often carrier mediated [36].

In order to evaluate if RPMI 2650 could be a representative model of the nasal mucosa, further investigation on the transporters expression in the cell line model was performed and was compared with freshly brushed human nasal cells.

Specifically, 47 xenobiotic transporters were investigated. The genes investigated were those expressing ATP Binding Cassette (ABC), Solute Carrier (SLC) and Solute Carrier Organic anion (SLCO) proteins. Table 1 graphically summarizes which of these 47 xenobiotic transporters were present in the RPMI 2650 cells and compared with gene present on PNC: human primary nasal cells from brushing (average between male and female).

(Table 1 Here)

For the RPMI 2650 cells, the highly expressed genes ($\Delta Cq<5$) were found to be MRP1 and MRP9 proteins while the poorly expressed genes ($\Delta Cq>15$) were found to be for the following transporters: BSEP (Bile Salt Export Pump), MRP5 (Multidrug Resistance-associated Protein 5), MRP7, MRP8, OCT3 (Organic Cation Transporter 3), CNT3 (Anti-Concentrative Nucleoside Transporter 3), ENT1 (Equilibrative nucleoside transporter 1) and ENT3. Some genes, such as those expressing MRP6, PEPT1 (Peptide transporter 1), PEPT2, NaPi1 (Renal type I sodium/phosphate transporter), OCT1, OCT2, URAT1 (Organic anion/urate transporter 1), ATB(0+) (Sodium- and chloride-dependent neutral and basic amino acid transporter B(0+)), OATP-C (Organic anion transporter polypeptide C), OATP-8, OATP-F, OATP-B were

not expressed at all. All the other genes were expressed at an intermediate level (5<ΔCq<15).

In terms of the primary nasal cells obtained by nasal mucosa brushing, no differences were found between male and female volunteers. Highly expressed genes were those encoding for the following transporter proteins: MDR3, MRP1, MRP9, MRP2, MRP3, MRP4, NTCP (Sodium-taurocholate cotransporting polypeptide), MCT1 (Monocarboxylate transporter 1), OCTN2 (Organic cation transporter, novel 2), CNT3, ENT1, ENT2 and OATP-H. No genes were classified as poorly expressed and only 11 genes were not expressed at all (MRP6, OCT1/2, OCTN1, OAT1/2/3, CNT1/2, ATB (0+) and OATP-F). Gene expressions were calculated using 18S rRNA as reference gene. Using a single reference gene could represent a limitation of the study, however, 18S rRNA has been indicated as the most suitable reference gene in qPCR normalization of data in the case of other primary human airways epithelial tissues [29].

Corticosteroids, which are one of the main topical nasal active ingredients, are an example of a drug class that is associated with these cell transporters [37,38]. In particular, budesonide and beclomethasone dipropionate (BDP) have shown effect of the expression of BCRP, PGP, OCT1 and OCT2 in Calu-3 and breast cancer cell lines [39,40]. In addition, budesonide has been found to be a substrate of P-glycoprotein (ABCB1) in transport experiments across Caco-2 cell line [41].

Nevertheless, to our knowledge there is a lack of information about their role in the nose [35]. Our data shows that BRCP and PGP are expressed in the nasal epithelium and in the RPMI 2650 model, suggesting that an avenue for future investigations in this direction.

Although the xenobiotic genes expression was found to be higher for primary cells than for RPMI 2650 in general, the same genes were expressed in both primary human mucosa nasal cells and RPMI 2650, highlighting the potential use of RPMI2650 grown on ALI as a suitable model for nasal mucosa. In addition, from the 47 genes that encode for transporter proteins, the 11 that were not expressed in primary cells were also absent in RPMI 2650, further supporting a good correlation between the RPMI 2650 cell model and human nasal mucosa. The following proteins: NaPi1, URAT1, PEPT1, PEPT2, OATP-C and OATP-8 were found to be expressed in brushed nasal cells, but not in RPMI 2650; this could be considered as a limitation to the RPMI 2650 model in terms of transport of peptides and organic anionic substances.

Kreft et al. had previously described the expression of some of xenobiotic transporter genes in RPMI 2650 grown in ALI conditions with two different culturing media and at two culturing time points: 1 and 3 weeks, without finding any relevant differences [20]. Our data correlate nicely with those published by Kreft, suggesting good reproducibility of RPMI2650 cell model.

Development and Validation of the Modified Expansion Chamber

The different materials used for the manufacturing of the FDA guideline expansion chamber (glass) and the 3D printed modified chamber (ABS) could raise the question whether or not the aerosol performances and particle deposition in the two chambers could be different. Therefore, in order to validate the 3D printed modified chamber, the aerosol performance of a commercially available nasal spray

(Rhinocort Nasal Spray, AstraZeneca, Australia) was evaluated using a NGI cascade impactor using both expansion chambers. Table 3 shows the percentage of budesonide (calculated as percentage of the emitted nominal dose, 96 µg) recovered in each stage of NGI after 3 actuations of the Rhinocort device (average of 3 runs), using both devices.

(Table 3 Here)

The amount of drugs in the 3D printed modified chamber was calculated as sum of the mass recovered from both the upper and lower hemisphere and the three Snapwells in the chamber. As expected, the majority of the drug was found in the chamber demonstrating that the device produced a coarse spray with an aerodynamic diameter that is higher than 10 µm, with minimal respirable fraction. Overall, there were no statistical differences in aerosol performance for Rhinicort between the modified and the glass chamber for all NGI stages (no drug was recovered for stages lower than 2). With the deposition onto the Snapwell inserts, 13.12 ± 0.07 µg of budesonide were recovered from the three cell inserts after the extraction with 80:20 (v/v) methanol/ water, with approximately 4.4 µg of budesonide on each well. This is equivalent to roughly 13.7% of the dose emitted with each spray of the Rhinocort suspension that reaches each Snapwell inserts.

Having validated the modified chamber in terms of aerosol performance, the RPMI 2650 cells grown on Snapwell inserts were introduced into the modified chamber in order to perform cells permeation experiments. The maintenance of barrier properties and the integrity of the cell layers are key factors for permeation studies. In order to confirm that the handling of the Snapwell inserts and the process of

deposition into the modified chamber were not hampering the barrier properties of RPMI 2650 nasal cell model, a solution of HBSS was sprayed 6 times on the RPMI2650 nasal cells into the chamber. The cells were removed from the chamber and after 4 hours of Flu-Na permeation studies, the P_{app} was calculated. No statistical differences were found ($p<0.05$) between the P_{app} values of control and treated cells.

Finally, deposition and permeation experiments were performed using a budesonide commercial spray and with the 3D printed modified expansion chamber connected to the cascade impactor, using the three Snapwells inserts with RPMI 2650 cells grown for 14 days. The formulation was deposited on the cells after device actuation and RMPI 2650 cells inserts were placed back in cell culture plates to perform the permeation study.

(Figure 7 Here).

Figure 7 shows the percentage of budesonide transported across the nasal cell model after deposition in the 3D MC; the In the first hour, approximately 47.3 ± 5.0 % of the drug was transported. This can be explained, as suggested by Baumann, due to the high quantity of available budesonide dissolved in the commercially available product to bind and diffuse readily through the epithelium [42,43]. At the end of the experiment (4 hours), 83.1 ± 6.3 % of the total drug deposited reached the basal compartment. Between three to four hours, a decreased permeation rate was observed, probably due to the depletion of budesonide on the surface of the cells that consequently decreases the gradient between the two compartments (apical

and basal). The total amount of budesonide found on each well was on average of 0.79 ± 0.25 µg. This was calculated from the sum of the budesonide on, in and transported across the cell layer; the total amount recovered from each well was used as 100% reference value for the calculation in the cell deposition/ transport studies. This variability of the amount of budesonide deposited on each well could be related to both the plume geometry of Rhinocort nasal spray and the manual activation of the device, that don't allow a uniform deposition on each well. The integrity of the cell layer was maintained within the time scaled study with no statistical differences ($p>0.05$) was found between TEER values before (126 ± 21 Ω•cm^2) and after (127 ± 14 Ω•cm^2) the transport studies.

As shown in Figure 8, after 4 hours 14.4 ± 4.9 % of the drug remains on the surface of the cell and 2.5 ± 1.6 % of budesonide was found inside the cells, suggesting low binding and internalization within the cells of the RPMI 2650 nasal mucosa model. This is in good agreement with data published by Baumann showing that lower levels of budesonide bind to human nasal tissue when compared with other glucocorticoids [42].

(Figure 8 Here)

CONCLUSION

This research has shown that RPMI 2650 cells could be successfully grown on Snapwell inserts. The cells form a continuous layer offering a permeation barrier similar in terms of trans-epithelial electrical resistance and sodium fluorescein paracellular permeation to previously reported nasal epithelium models and more

importantly to excised human nasal mucosa. It was also shown that RPMI 2650 cells produce mucus and its production is related to seeding density and time in culture. The optimal conditions for RPMI 2560 to achieve the highest epithelial barrier and a complete coating with mucus layer are: Snapwell polycarbonate inserts at seeding density of 2.50 x10^6 cell/ml and cultured for 14 days in ALI culture. Regarding protein transporters expression, RPMI 2650 cells represent a good model of the nasal epithelium, correlating well with gene expression of freshly collected human nasal epithelial cells. A 3D printed modified expansion chamber, which allow deposition of nasal formulation directly on RPMI 2650 grown on Snapwell inserts has been successfully designed, validated and tested using a commercial nasal spray, showing that this model could be used concomitantly to study nasal formulations aerosol deposition and permeation through a nasal epithelium model of the aerosolized formulation.

Acknowledgements

A/Professor Traini is the recipient of an Australian Research Council Future Fellowship (project number FT12010063). A/Professor Young is the recipient of an Australian Research Council Future Fellowship (project number FT110100996).

Author Disclosure Statements

No conflicts of interest exist.

References

[1] L. Illum, Nasal drug delivery — Recent developments and future prospects, J. Control. Release. 161 (2012) 254–263.

[2] M. Pozzoli, P. Rogueda, B. Zhu, T. Smith, P.M. Young, D. Traini, F. Sonvico. Dry Powder Nasal Drug Delivery: Challenges, Opportunities and a study of the commercial Teijin Puvlizer Rhinocort® device and formulation, Drug Dev. Ind. Pharm. (2016) doi: 10.3109/03639045.2016.1160110.

[3] V. Saluja, J.P. Amorij JP, M.L. van Roosmalen, K. Leenhouts, A. Huckriede, W.L.J. Hinrichs, H.W. Frijlink, Intranasal delivery of influenza subunit vaccine formulated with GEM particles as an adjuvant. AAPS J. 12 (2010) 109–16.

[4] S. Grassin-Delyle, A. Buenestado, E. Naline, C. Faisy, S. Blouquit-Laye, L.J. Couderc, M. Le Guen, M. Fischler, P. Devillier, Intranasal drug delivery: an efficient and non-invasive route for systemic administration: focus on opioids, Pharmacol. Ther. 134 (2012) 366–379.

[5] E. Touitou, L. Illum, Nasal drug delivery. Drug Deliv. Transl. Res. 3 (2013) 1–3.

[6] H. Wu, K. Hu, X. Jiang X, From nose to brain: understanding transport capacity and transport rate of drugs, Expert Opin. Drug Deliv. 5 (2008)1159–68.

[7] M.S. Quraishi, N.S. Jones, J.D. Mason, The nasal delivery of drugs, Clin. Otolaryngol. Allied Sci. 22 (1997) 289–301.

[8] P.G. Djupesland, Nasal drug delivery devices: characteristics and performance in a clinical perspective—a review, Drug Deliv. Transl. Res. 3 (2013) 42–62.

[9] C. Comfort, G. Garrastazu, M. Pozzoli, F. Sonvico, Opportunities and Challenges for the Nasal Administration of Nanoemulsions. Current Topics Med. Chem. 15 (2015) 356–68.

[10] F. Merkus, J. Verhoef, N. Schipper, E. Marttin, Nasal mucociliary clearance as a factor in nasal drug delivery, Adv Drug Deliv Rev. 29 (1998) 13–38.

[11] Great Britain SO. British Pharmacopoeia. London: Stationery Office; Appendix XII C. Consistency of Formulated Preparations.

[12] CDER F. Bioavailability and Bioequivalence Studies for Nasal Aerosols and Nasal Sprays for Local Action. 2003;1–37.

[13] W.H. Doub, W.P. Adams, A. M. Wokovich, J.C. Black, M. Shen, L.F. Buhse, Measurement of Drug in Small Particles from Aqueous Nasal Sprays by Andersen Cascade Impactor, Pharm Res. 29 (2012) 3122–3130.

[14] M. Haghi, D. Traini, P. Young. *In vitro* cell integrated impactor deposition methodology for the study of aerodynamically relevant size fractions from commercial pressurised metered dose inhalers, Pharm. Res. 31 (20149 1779–1787.

[15] C.I. Grainger, L.L. Greenwell, G.P. Martin, B. Forbes, The permeability of large

molecular weight solutes following particle delivery to air-interfaced cells that model the respiratory mucosa, Eur. J. Pharm. Biopharm. 71 (2009) 318–324.

[16] M. Bur, B. Rothen-Rutishauser, H. Huwer, C.M. Lehr, A novel cell compatible impingement system to study in vitro drug absorption from dry powder aerosol formulations, Eur. J. Pharm. Biopharm. 72 (2009) 350–357.

[17] A. De Fraissinette, R. Brun, H. Felix, J. Vonderscher, A. Rummelt, Evaluation of the human cell line RPMI 2650 as an in vitro nasal model, Rhinology 33 (1995) 194–198.

[18] A. Wengst, S. Reichl, RPMI 2650 epithelial model and three-dimensional reconstructed human nasal mucosa as in vitro models for nasal permeation studies, Eur. J. Pharm. Biopharm. 74 (2010) 290–297.

[19] S. Bai, T. Yang, T.J. Abbruscato, F. Ahsan, Evaluation of human nasal RPMI 2650 cells grown at an air-liquid interface as a model for nasal drug transport studies, J. Pharm. Sci. 97 (2007) 1165–1178.

[20] M.E. Kreft, U.D. Jerman, E. Lasič, T. Lanišnik Rižner, N. Hevir-Kene, L. Peternel, K. Kristan, The Characterization of the Human Nasal Epithelial Cell Line RPMI 2650 Under Different Culture Conditions and Their Optimization for an Appropriate in vitro Nasal Model, Pharm. Res. 32 (2015) 665-679.

[21] S. Reichl, K. Becker, Cultivation of RPMI 2650 cells as an *in vitro* model for human transmucosal nasal drug absorption studies: optimization of selected culture conditions, J. Pharm. Pharmacol. 64 (2012) 1621–1630.

[22] D.D. Kim, *In Vitro* Cellular Models for Nasal Drug Absorption Studies in C. Ehrhardt, K.J. Kim (Eds.) Drug Absorption Studies *In Situ, In Vitro and In Silico* Models, Springer, New York, 2008, pp. 216–234.

[23] M. Hagi, P.M. Young, D. Traini, R. Jaiswal, J. Gong, M. Bebawy, Time- and passage-dependent characteristics of a Calu-3 respiratory epithelial cell model. Drug Dev. Ind. Pharm. 36 (2010) 1207–1214.

[24] C.A. Schneider, W.S. Rasband, K.W. Eliceiri, NIH Image to ImageJ: 25 years of image analysis, Nat Methods. 9 (2012) 671–675.

[25] L.A. Clarke, L. Sousa, C. Barreto, M.D Amaral, Changes in transcriptome of native nasal epithelium expressing F508del-CFTR and intersecting data from comparable studies, Respir. Res. 14 (2013) 38.

[26] S. Beck, D. Penque, S. Garcia, A. Gomes, C. Farinha, L. Mata, S. Gulbenkian, K. Gil-Ferreira, A. Duarte, P. Pacheco, C. Barreto, B. Lopes, J. Cavaco, J. Lavinha, M.D. Amaral, Cystic fibrosis patients with the 3272-26A-->G mutation have mild disease, leaky alternative mRNA splicing, and CFTR protein at the cell membrane, Hum. Mutat. 14 (1999) 133–144.

[27] C.M. Harris, F. Mendes, A. Dragomir, I.J.M. Doull, I. Carvalho-Oliveira, Z. Bebok, J.P. Clancy, V. Eubanks, E.J. Sorscher, G.M. Roomans, M.D. Amaral, M.A. McPherson , D. Penque, R.L. Dormer, Assessment of CFTR localisation in native

airway epithelial cells obtained by nasal brushing, J Cyst. Fibros. 3 (2004) 43–48.

[28] H.X. Ong, D. Traini, G. Ballerin, L. Morgan, L. Buddle, S. Scalia, P.M. Young. Combined inhaled salbutamol and mannitol therapy for mucus hyper-secretion in pulmonary diseases, AAPS J. 16 (2014) 269–280.

[29] S.V. Kuchipudi, M. Tellabati, R.K. Nelli, G.A. White, B.B. Perez, S. Sebastian, M.J. Slomka, S.M. Brookes, I.H. Brown IH, S.P. Dunham, K.C. Chang, 18S rRNA is a reliable normalisation gene for real time PCR based on influenza virus infected cells, Virol. J. 9 (2012) 230.

[30] S.R. Naikwade, A.N. Bajaj, Development of validated specific HPLC method for budesonide and characterization of its alkali degradation product, Can. J. Anal. Sci. Spect. 53 (2008) 113–122.

[31] C.U. Cotton, M.J. Stutts, M.R. Knowles,J.T. Gatzy, R.C. Boucher. Abnormal apical cell membrane in cystic fibrosis respiratory epithelium. An *in vitro* electrophysiologic analysis, J. Clin. Invest. 79 (1987) 80–85.

[32] J.D. Suman, Current understanding of nasal morphology and physiology as a drug delivery target, Drug Deliv. Transl. Res. 3 (2013) 4–15.

[33] V.S. Subramanian, J.S. Marchant, D. Ye, T.Y. Ma, H.M. Said HM, Tight junction targeting and intracellular trafficking of occludin in polarized epithelial cells, AJP: Cell Physiology. 293 (2007) C1717–1726.

[34] J.J. Salomon, V.E. Muchitsch, J.C. Gausterer, E. Schwagerus, H. Huwer, N. Daum N, C.M. Lehr, C. Ehrhardt, The Cell Line NCl-H441 Is a Useful *in Vitro* Model for Transport Studies of Human Distal Lung Epithelial Barrier, Mol. Pharm. 11 (2014) 995-1006.

[35] S. Nickel, C.G. Clerkin, M.A. Selo, C. Ehrhardt, Transport mechanisms at the pulmonary mucosa: implications for drug delivery, Expert Opin. Drug Deliv. 13 (2016) 667-690.

[36] K. Bleasby, J.C. Castle, C.J. Roberts, C. Cheng, W.J. Bailey, J.F. Sina JF, A.V. Kulkarni, M.J. Hafey, R. Evers, J.M. Johnson, R.G. Ulrich, J.G. Slatter, Expression profiles of 50 xenobiotic transporter genes in humans and pre-clinical species: a resource for investigations into drug disposition. Xenobiotica. 36 (2006) 963–988.

[37] A.J. Trangsrud, A.L. Whitaker, R.E. Small. Intranasal corticosteroids for allergic rhinitis. Pharmacotherapy. 22 (2002) 1458–1467.

[38] W.E. Berger, J.W. Godfrey, A.L. Slater, Intranasal corticosteroids: the development of a drug delivery device for fluticasone furoate as a potential step toward improved compliance, Expert Opin. Drug Deliv. 4 (2007) 689–701.

[39] K.O. Hamilton, M.A. Yazdanian, K.L. Audus, Modulation of P-glycoprotein activity in Calu-3 cells using steroids and beta-ligands, Int. J. Pharm. 228 (2001) 171–179.

[40] H.C. Cooray, S. Shahi, A.P. Cahn, H.W. van Veen, S.B. Hladky, M.A. Barrand,

Modulation of p-glycoprotein and breast cancer resistance protein by some prescribed corticosteroids, Eur. J. Pharmacol. 531 (2006)25–33.

[41] K. Dilger, M. Schwab, M.F. Fromm, Identification of budesonide and prednisone as substrates of the intestinal drug efflux pump P-glycoprotein, Inflamm. Bowel Dis. 10 (2004) 578–583.

[42] D. Baumann, C. Bachert, P. Högger, Development of a novel model for comparative evaluation of intranasal pharmacokinetics and effects of anti-allergic nasal sprays, Eur J Pharm Biopharm. 80 (2012) 156–163.

[43] D. Baumann, C. Bachert, P. Högger, Dissolution in nasal fluid, retention and anti-inflammatory activity of fluticasone furoate in human nasal tissue *ex vivo*, Clin. Exp. Allergy. 39 (2009) 1540–1550.

Table(s)

Table 1. List of drug transporters evaluated and their gene expression (ΔCq) in RPMI2650 cultivated on Snapwells at 2.50 x10^6 cell/ml, PNC: human primary nasal cells from brushing (average between male and female). Scale from not expressed (red) to highly expressed (dark green)

Protein Name	Protein Description	Gene code	RPMI 2650	PNC	ΔCq	Classification
P-gp	P-glycoprotein	ABCB1			30	No Expression
BSEP	Bile Salt Export Pump	ABCB11			15 to30	Poorly Expressed
MDR3	Multidrug resistance protein 3	ABCB4			5 to 15	Expressed
MRP1	Multidrug resistance-associated protein 1	ABCC1			<5	Highly Expressed
MRP7	Multidrug resistance-associated protein 7	ABCC10				
MRP8	Multidrug resistance-associated protein 8	ABCC11				
MRP9	Multidrug resistance-associated protein 9	ABCC12				
MRP2	Multidrug resistance-associated protein 2	ABCC2				
MRP3	Multidrug resistance-associated protein 3	ABCC3				
MRP4	Multidrug resistance-associated protein 4	ABCC4				
MRP5	Multidrug resistance-associated protein	ABCC5				
MRP6	Multidrug resistance-associated protein 6	ABCC6				
BCRP	breast cancer resistance protein	ABCG2				
NTCP	Sodium-taurocholate cotransporting polypeptide	SLC10A1				
PEPT1	Peptide transporter 1	SLC15A1				
PEPT2	Peptide transporter 2	SLC15A2				
MCT1	Monocarboxylate transporter 1	SLC16A1				
MCT2	Monocarboxylate transporter 2	SLC16A7				
NaPi1	Renal type I sodium/phosphate transporter	SLC17A1				
(OCT1)	Organic cation transporter 1	SLC22A1				
URAT1	Organic anion/urate transporter 1	SLC22A12				
(OCT2)	Organic cation transporter 2	SLC22A2				
(OCT3)	Organic cation transporter 3	SLC22A3				
OCTN1	Organic cation transporter, novel 1	SLC22A4				
OCTN2	Organic cation transporter, novel 2	SLC22A5				

OAT1	Organic anion transporter 1	SLC22A6		
OAT2	Organic anion transporter 2	SLC22A7		
OAT3	Organic anion transporter 3	SLC22A8		
CNT1	Anti-Concentrative Nucleoside Transporter 1	SLC28A1		
CNT2	Anti-Concentrative Nucleoside Transporter 2	SLC28A2		
CNT3	Anti-Concentrative Nucleoside Transporter 3	SLC28A3		
ENT1	Equilibrative nucleoside transporter 1	SLC29A1		
ENT2	Equilibrative nucleoside transporter 2	SLC29A2		
ENT3	Equilibrative nucleoside transporter 3	SLC29A3		
ENT4	Equilibrative nucleoside transporter 4	SLC29A4		
OSTα	Organic Solute Transporter, Alpha	SLC51A		
ATB(0+)	Sodium- and chloride-dependent neutral and basic amino acid transporter B(0+)	SLC6A14		
OATP-A	Organic anion transporter polypeptide A	SLCO1A2		
OATP-C	Organic anion transporter polypeptide C	SLCO1B1		
OATP-8	Organic anion transporter polypeptide 8	SLCO1B3		
OATP-F	Organic anion transporter polypeptide F	SLCO1C1		
PGT	Prostaglandin Transporter	SLCO2A1		
OATP-B	Organic anion transporter polypeptide B	SLCO2B1		
OATP-D	Organic anion transporter polypeptide D	SLCO3A1		
OATP-E	Organic anion transporter polypeptide E	SLCO4A1		
OATP-H	Organic anion transporter polypeptide H	SLCO4C1		
OATP-J	Organic anion transporter polypeptide J	SLCO5A1		

Table 2. P_{app} values ($x10^{-6}$ cm/s) of Flu-Na across RPMI 2650 cultured in ALI conditions for three different seeding densities (n=3; $\pm$ StDev) compared to values obtained for excised human nasal mucosa

Flu-Na P_{app} values ($x10^{-6}$ cm/s)				
Seeding Density	1.25 ($x10^6$ cells/ml)	2.50 ($x10^6$ cells/ml)	5.00 ($x10^6$ cells/ml)	Human Nasal Mucosa
Freshly excised	-	-	-	3.12 ± 1.99 [18]
Week 1	5.32±0.37	5.21±0.27	5.47±0.49	
Week 2	3.67±0.21	2.68±0.60	2.95±0.17	
Week 3	3.47±0.20	3.55±0.30	2.69±0.18	

Table 3. Amount of Budesonide (% of nominal dose) recovered from each Stage of the NGI using the Glass and Modified chamber (n=3 ± StDev).

	Chamber	Connection Tube	Stage 1	Stage 2*
Glass Chamber	98.75±0.09	0.57±0.05	0.50±0.03	0.18±0.04
Modified Chamber	98.73±0.09	0.57±0.07	0.51±0.03	0.19±0.01

* No Budesonide was found below Stage 2

Figure captions

Figure 1. 3D drawing of the modified expansion chamber.

Figure 2. British Pharmacopoeia apparatus E equipped with FDA glass expansion chamber (A) and modified expansion chamber (B).

Figure 3. TEER of three different seeding densities of RPMI2650 cells cultured in the ALI conditions over time (n=3; ± StDev).

Figure 4. Optical microscope images of Alcian blue mucus staining on RPMI 2650 grown on Snapwell® inserts at 2.50 x10^6 cell/ml seeding density.

Figure 5. RGBb ratio values obtained after mucus staining as function of time in culture for the three different cell seeding densities (n=3; ± StDev).

Figure 6. Confocal Microscope Images of RPMI 2650 cells tight junction proteins-stained in green: E-cadherin (A) and ZO-1 (B-C). The blue and red colours in A and B respectively represent the DAPI staining of nuclei. C, the cross section of cell layers during confocal imaging: green ZO-1 and red cell nucleus.

Figure 7. Amount of budesonide transported through RPMI 2650 nasal cell model after NGI aerosols deposition using the 3D modified chamber (n=5 ± StDev).

Figure 8. Distribution of the budesonide recovered at the end of the experiment (4 hours) after the aerosol deposition using the 3D the modified expansion chamber (n=5 $\pm$ $StDev$).

Figure 1

Click here to download high resolution image

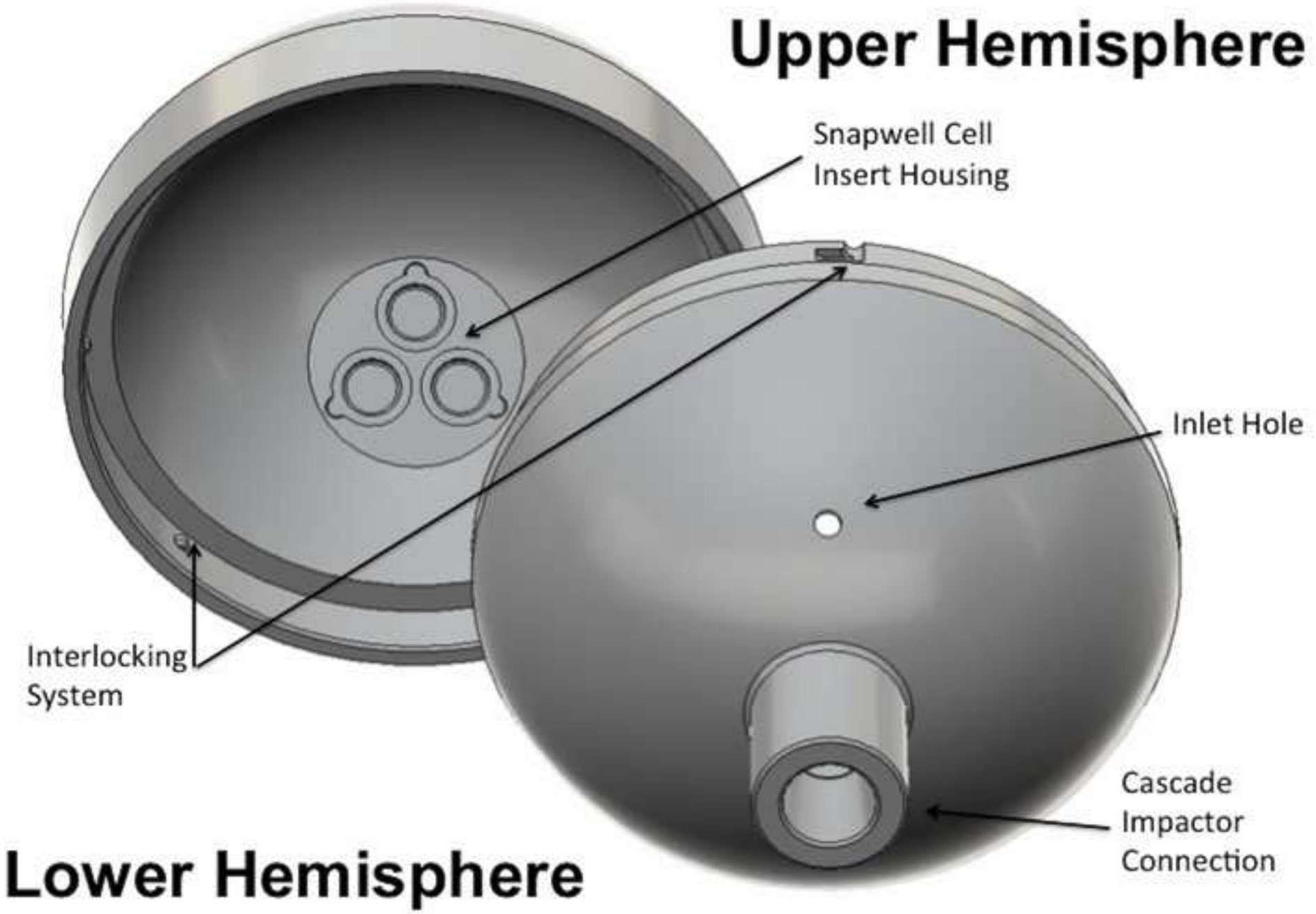

Figure 2

Click here to download high resolution image

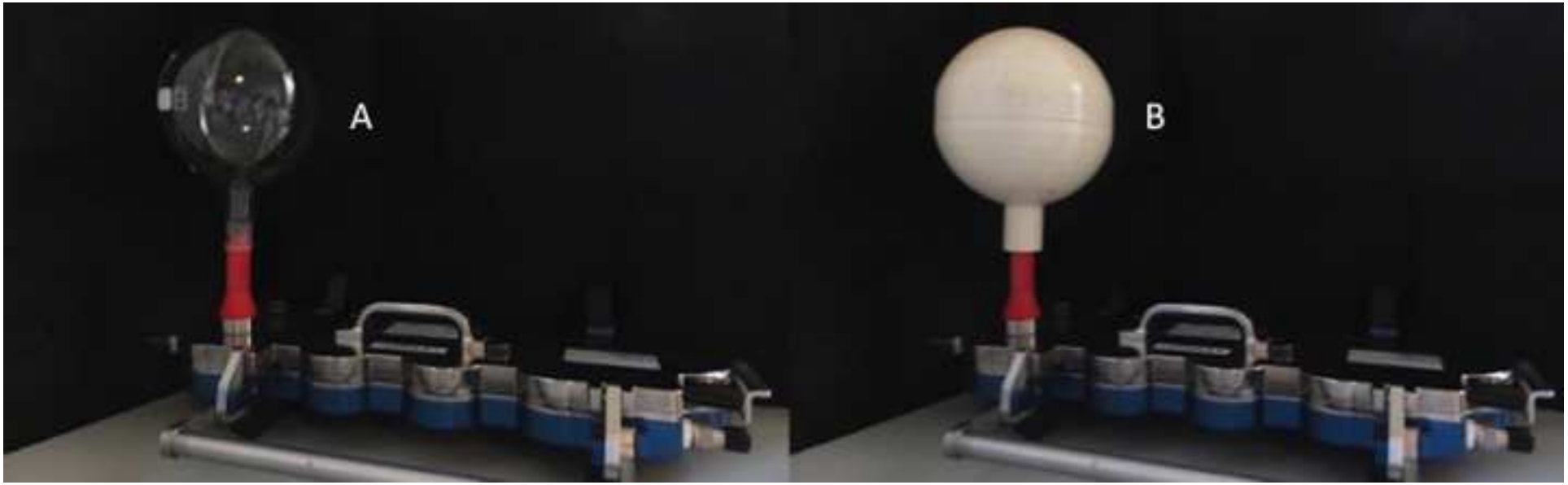

Figure3

Click here to download high resolution image

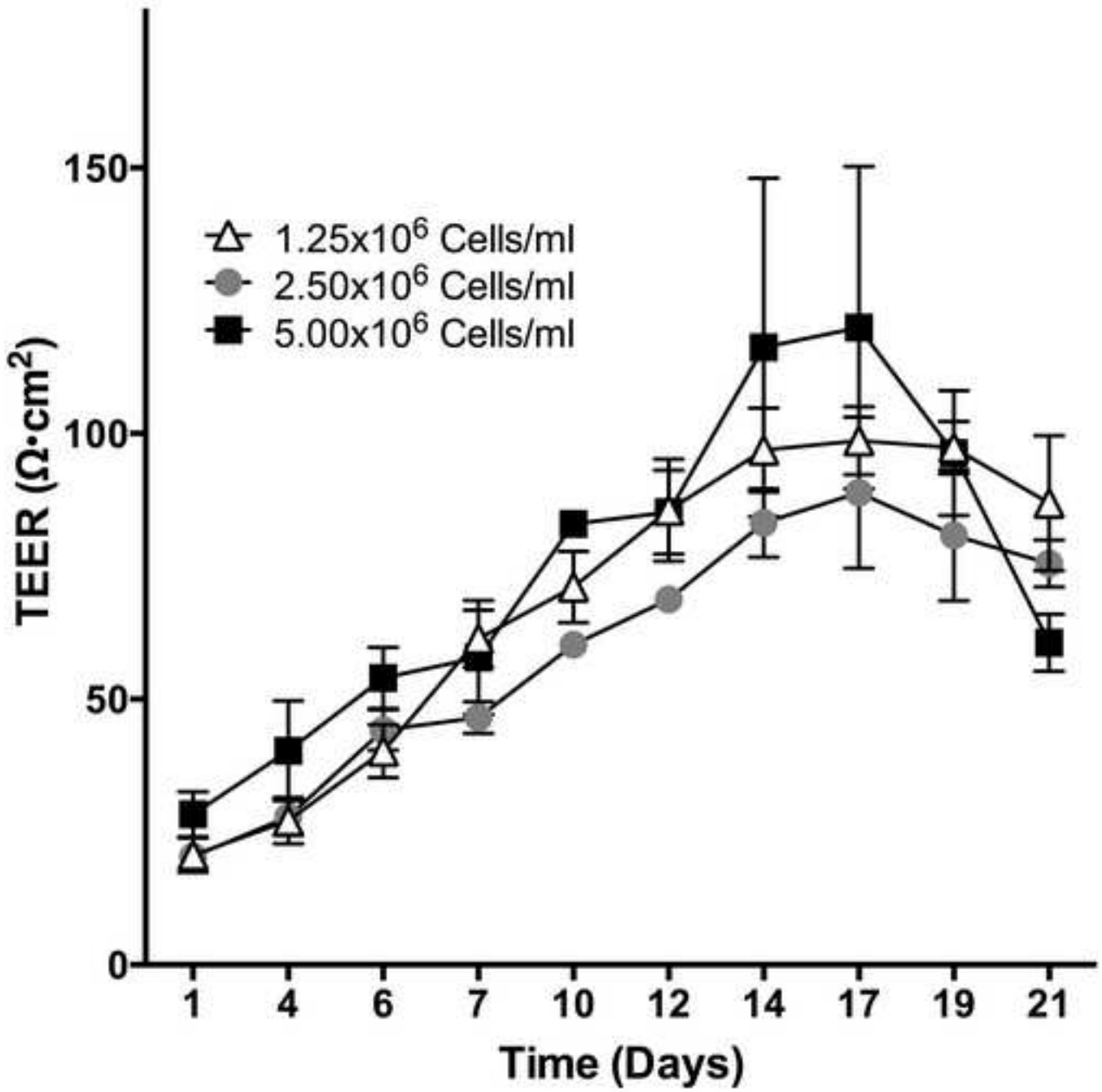

Figure 4

Click here to download high resolution image

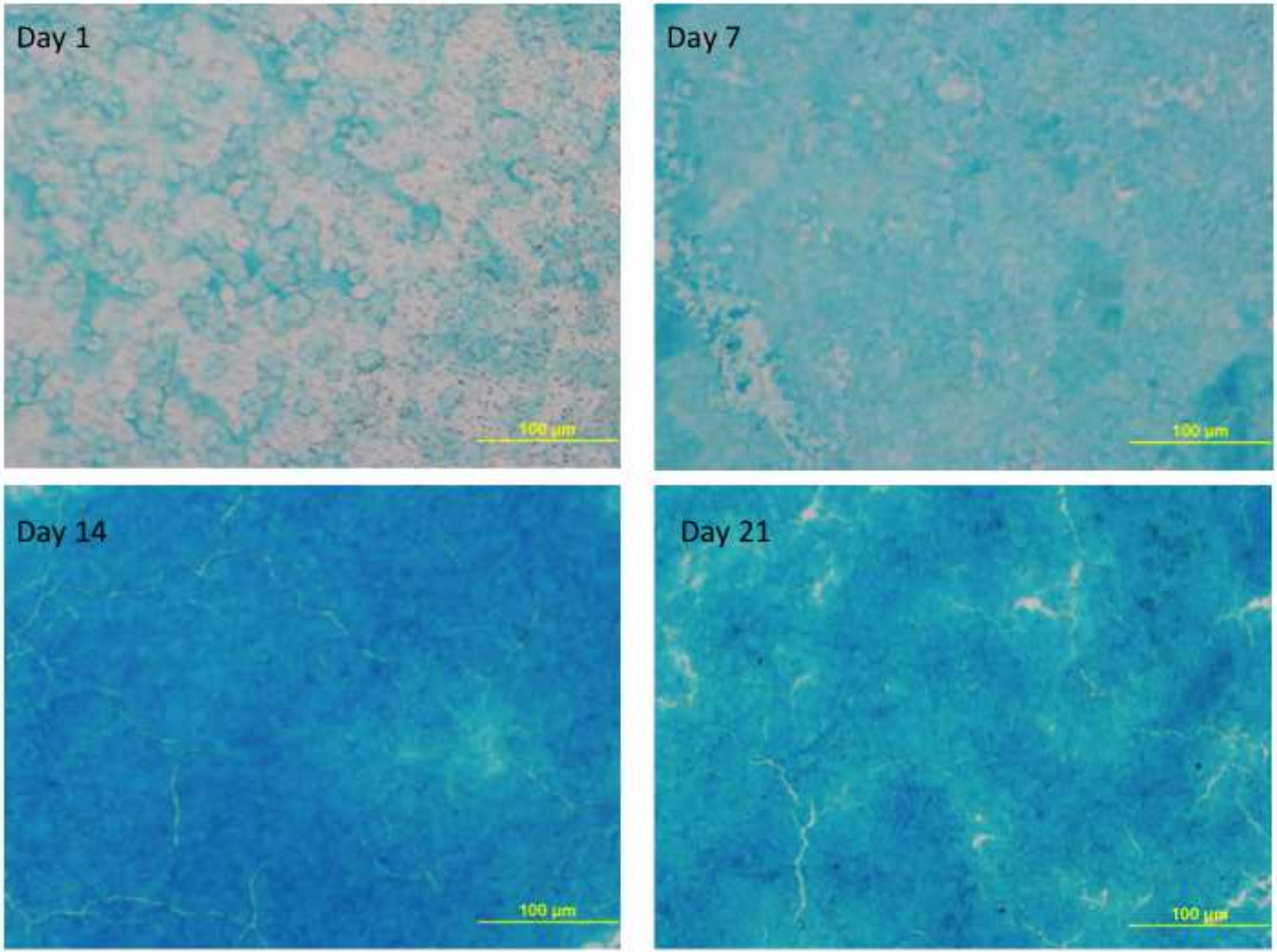

Figure 5

Click here to download high resolution image

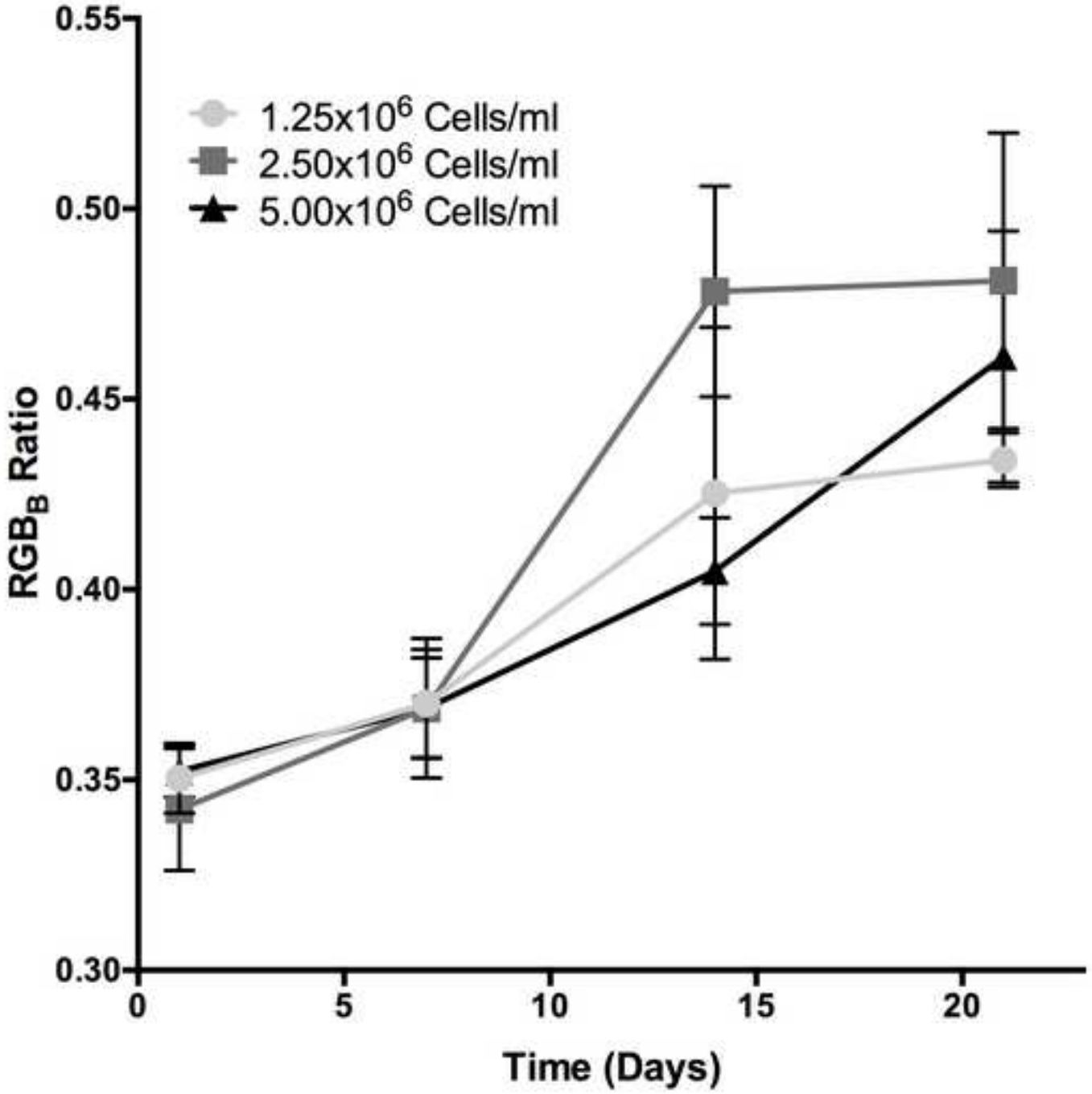

Figure 6

Click here to download high resolution image

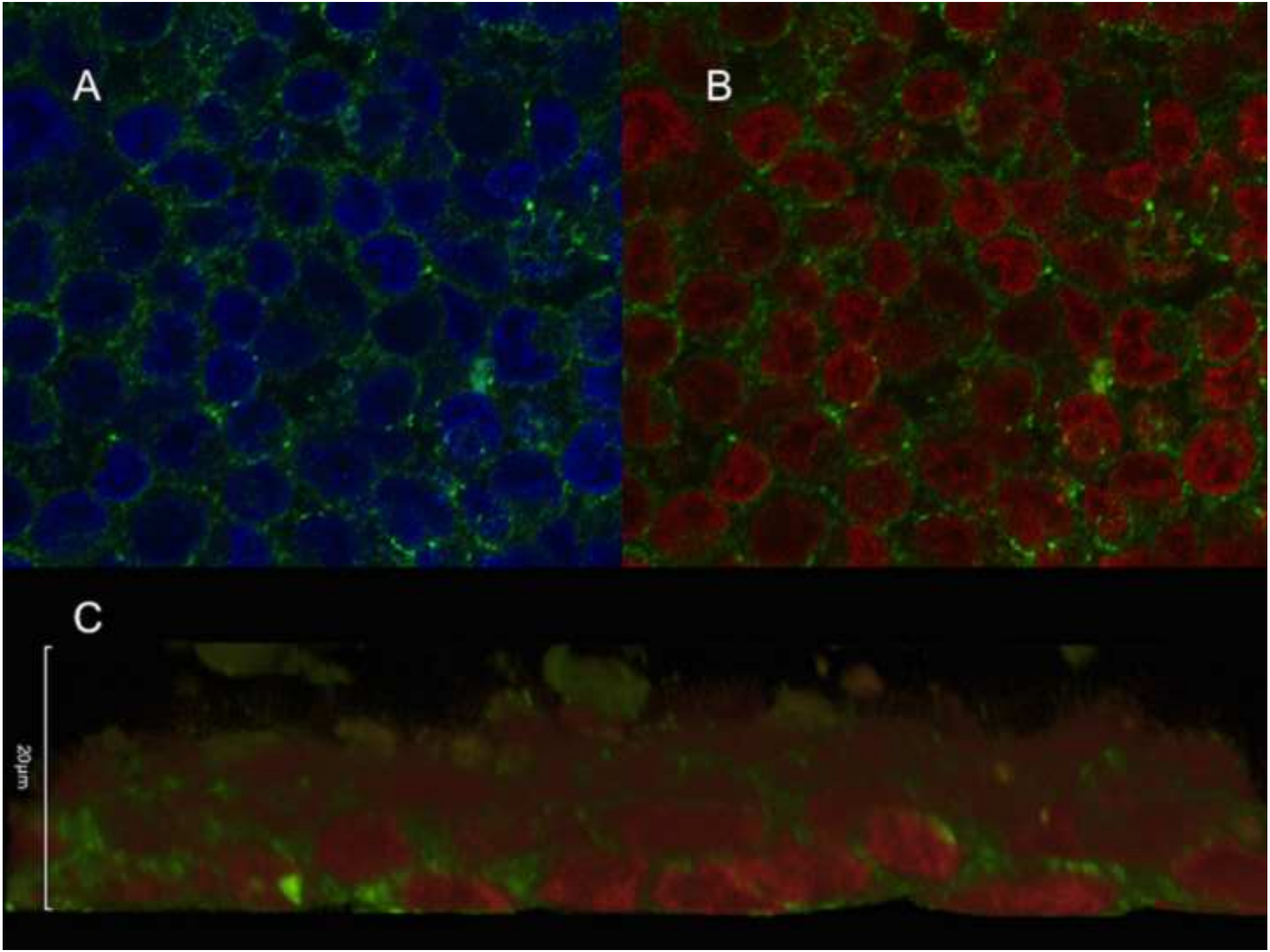

Figure 7

Click here to download high resolution image

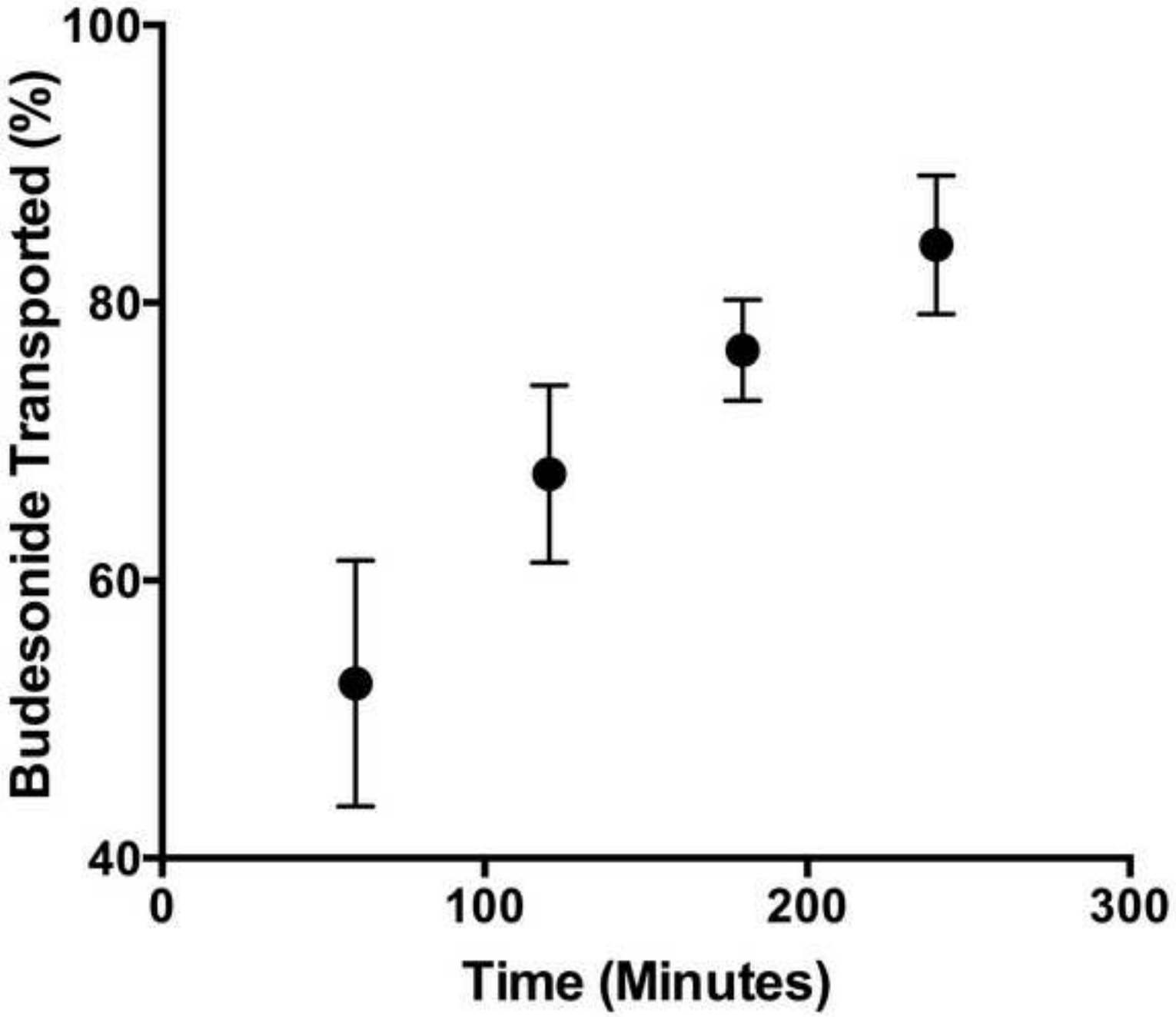

Figure 8

Click here to download high resolution image